Opto-Electronic Advances

Supplementary information

2021, Vol. 4, No. 2

DOI: 10.29026/oea.2021.200031

Generation of super-resolved optical needle and multifocal array using graphene oxide metalenses

Hongtao Wang[1,2,3,4†], Chenglong Hao[3†], Han Lin[1], Yongtian Wang[2], Tian Lan[2*], Chengwei Qiu[3*] and Baohua Jia[1*]

[1]Centre for Translational Atomaterials, Faculty of Science, Engineering and Technology, Swinburne University of Technology, P.O. Box 218, Hawthorn VIC 3122, Australia; [2]Key Laboratory of Photoelectronic Imaging Technology and System, Ministry of Education of China, School of Optics and Photonics, Beijing Institute of Technology, Beijing 100081, China; [3]Department of Electrical and Computer Engineering, National University of Singapore, 4 Engineering Drive 3, Singapore 117583, Singapore; [4]Engineering Product Development Pillar, Singapore University of Technology and Design, 8 Somapah Road, 487372, Singapore..

[†]These authors contributed equally to this work.

[*]Correspondence: E-mail: lantian@bit.edu.cn; E-mail: chengwei.qiu@nus.edu.sg; E-mail: bjia@swin.edu.au

Supplementary information for this paper is available at https://doi.org/10.29026/oea.2021.200031

S 1.1 The graphene oxide metalenses phase-amplitude dependency

When a uniform planewave ($E_0(r_1)=1$) illuminates the GO metalens, the beam is absorbed and refracted by GO/RGO zones, experiencing both amplitude and phase modulations. Based on the Beer-Lambert equations[1], the amplitude modulation becomes,

$$Amp=\sqrt{\mathrm{e}^{-\alpha(r_1)t(r_1)}} \tag{S1}$$

where $\alpha(r_1)$ is the absorption coefficient which can be calculated from extinction coefficient $K(r_1)$ through $\alpha(r_1)=4\pi\times K(r_1)/\lambda$. The $t(r_1)$ is the thickness of GO lens at position r_1 on GO metalens. The phase modulation can be calculated by optical path length, which is,

$$Phi=\frac{2\pi}{\lambda}\times n(r_1)\,t(r_1) \tag{S2}$$

where, the modulated refractive index $n(r_1)$, thickness $t(r_1)$, and extinction coefficient $K(r_1)$ due to the laser photo-reduction, can be formulated as,

$$\begin{cases} n(r_1)=n_{\mathrm{GO}}+\Delta n\cdot M(r_1) \\ t(r_1)=t_{\mathrm{GO}}+\Delta t\cdot M(r_1) \\ K(r_1)=K_{\mathrm{GO}}+\Delta K\cdot M(r_1) \end{cases} \tag{S3}$$

Here n_{GO}=2.01 is the refractive index of the GO film at 632.8 nm. t_{GO}=200 nm is the thickness of the GO film. K_{GO} = 0.078 is the extinction coefficient of GO at 632.8 nm. All these parameters are measured experimentally. The modulation function M can be expressed as a Gaussian function, continuous function ranged from 0 to 1.

$$M(r_1)=\sum_{m=1}^{N}\mathrm{e}^{\frac{(r_1-a_m)^2}{2w^2}} \tag{S4}$$

where, a_{m} is the position of m^{th} RGO zones, while w is the full width at a half maximum (FWHM) of rings.

The phase-amplitude relationship can be expressed as,

$$\frac{Amp^2}{Phi}=\frac{\exp\left(-\frac{4\pi}{\lambda}K(r_1)\cdot t(r_1)\right)}{\frac{2\pi}{\lambda}n(r_1)\,t(r_1)}=\frac{\exp(C\cdot Phi)}{Phi}\Rightarrow\begin{cases} Amp^2=\exp(C\cdot Phi) \\ C=-2\dfrac{K_{\mathrm{GO}}+(\Delta K/\Delta t)(t-t_{\mathrm{GO}})}{n_{\mathrm{GO}}+(\Delta n/\Delta t)(t-t_{\mathrm{GO}})} \end{cases} \tag{S5}$$

where, Amp and Phi are amplitude and phase modulations, respectively. Here, the parametric equation C is the function of thickness t, which ranges from t_{RGO} to t_{GO}. Therefore, the beam shape does not affect the phase-amplitude relationship. In other words, when the GO/RGO pair is determined, the transitional route is uniquely determined regardless of modulation function M. One way to think this intuitively is the thickness of intermediate RGO is fixed, the n, K value is also uniquely determined, thus, the phase-amplitude relationship for this intermediate RGO is uniquely determined.

The Taylor series can be applied to $(C\cdot Phi)$ in Eq. (S5), which yields,

$$Amp^2=1+C\cdot Phi+\frac{(C\cdot Phi)^2}{2!}+\frac{(C\cdot Phi)^3}{3!}+\cdots+\frac{(C\cdot Phi)^n}{n!}+\cdots \tag{S6}$$

when first five terms in Eq. (S6) are retained, this approximate equation can be expressed as,

$$Amp^2=1+C\cdot Phi+\frac{(C\cdot Phi)^2}{2}+\frac{(C\cdot Phi)^3}{6}+\frac{(C\cdot Phi)^4}{24}+\frac{(C\cdot Phi)^5}{120} \tag{S7}$$

The maximum error for transitional route 1 between Eq. (S5) and Eq. (S7) is only 0.2%, the routes comparison is shown in Fig. S2. From the Fig. S1 and 0.2% error, we can conclude that this polynomial equation is a very good approximation of phase-amplitude dependency in real applications.

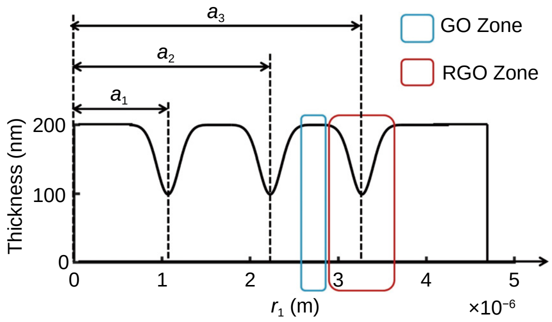

Appendix Fig. S1 | Schematic of the lens design

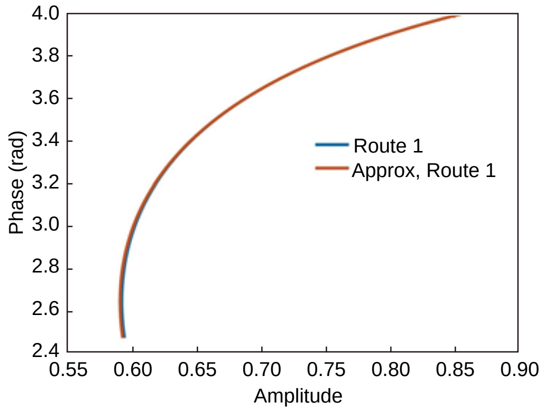

Appendix Fig. S2 | Comparison of route 1 and approximate Route 1 by polynomial equation (Eq. (S7)).

S 1.2 The phase-amplitude modulation and efficiency analysis of GO metalenses

In Fig S3(a), the GO film is reduced by femtosecond laser into RGO region. Thickness of RGO is about 100 nm and the grove profiles are Gaussian profiles. In direct femtosecond laser reduction process, the extinction and refractive index increase, and the thickness reduces. The specific values for GO/RGO and the thickness change caused by laser reduction are considered and calculated holistically. The phase and amplitude modulations are achieved by effective optical path difference for phase modulation and absorption for amplitude modulation. The refractive index and the extinction coefficient of reduced graphene oxide are 2.4894 and 0.5232 at the designed wavelength, while the ones of graphene oxide are 2.0138 and 0.0779. Then by using the Eq. S1 and Eq. S2, we can calculate the amplitude, which changes from 0.8567 to 0.5949. By taking air environment into consideration, the phase modulation is 0.1700π. These phase and amplitude modulation plots are shown in Fig S3(a).

Compared with the top-hat profile GO metalens, both focusing intensity and lateral resolution of Gaussian profile GO metalens are higher (Fig. S3(b)), which is the simulation results of two metalenses with the same focal length (FL) and numerical aperture (NA) using GO/RGO pair 1 and transitional route 1 in Fig. 1(d). The FL and NA for both GO metalenses are 15 μm and 0.747, respectively. The point spread function (PSF) of the top-hat profile GO metalens has a higher side lobe along the axial direction, and the lateral resolution is 468 nm compared with 427 nm of the Gaussian profile GO metalens. It proves that, Gaussian profile GO lens performs better than top-hat profile GO lens in focal resolution (the focal spot size).

For the ease of efficiency analysis, we take 1D GO gratings with Gaussian and top-hat surface profiles for comparison. The diffraction efficiency (DE) comparison for 1D GO grating with two profiles are theoretically calculated via Fourier series decomposition[2]:

$$\begin{aligned} C_m &= \frac{1}{T}\int_{-T/2}^{T/2} A\exp(i\varphi)\cdot\exp\left(-i2\pi m\frac{x}{T}\right)\mathrm{d}x \\ \eta &= |C_m|^2 \end{aligned} \tag{S8}$$

where, C_{m} is coefficient of m^{th} order, T is grating period, and η is the DE. A and φ representing for Gaussian surface can be expressed by Eq. S4. Meanwhile, A and φ from top-hat surface are exactly the ones from GO/RGO pair 1 in Fig. S3(b).

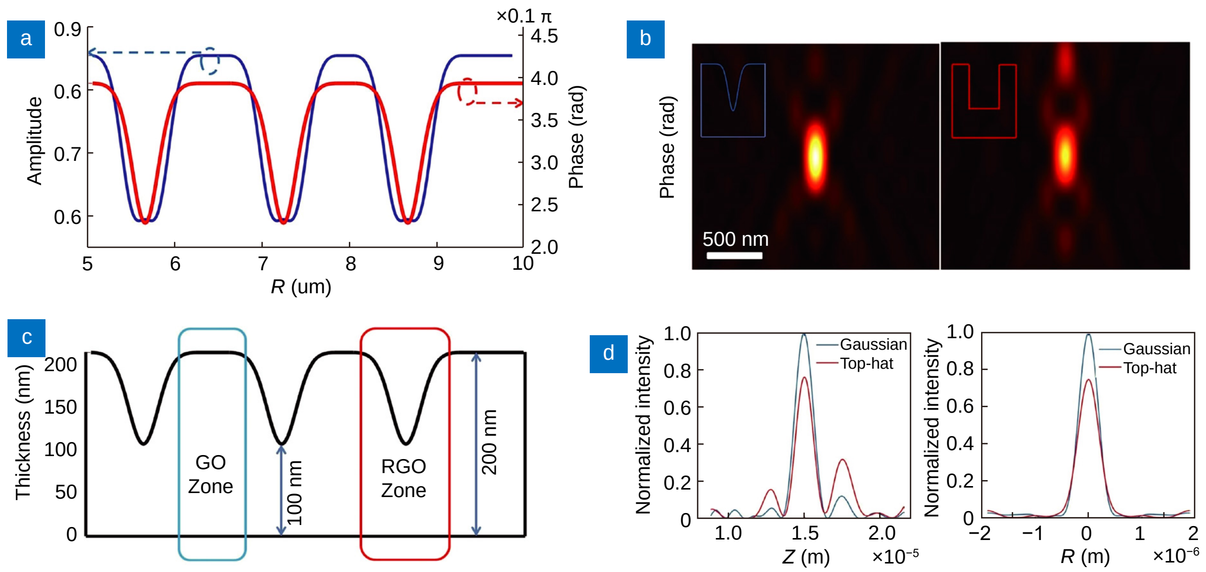

Appendix Fig. S3 | (a) Schematic of the phase and modulations of GO metalenses and (b) comparison between Gaussian profile GO metalens and top-hat profile GO metalens.

The T is 800 nm in our calculation, the duty cycle of the gratings is 0.5. The calculated zero-order and first-order DE from Gaussian profile gratings are 43.17% and 44.05%, respectively. In comparison, the calculated zero-order and first-order DE from top-hat profile gratings are 49.14% and 2.13%, respectively. It can be concluded that the 1D GO gratings with a Gaussian surface profile have a better first-order DE, which is primarily used for focusing. The statement stays true in the case of 2D GO metalenses, the calculated efficiency is 19.6%. In conclusion, Gaussian profile GO metalenses perform better than Top-hat profile GO metalens in both resolution (the focal spot size) and efficiency.

S 1.3 The influence of GO film fluctuation on optical modulation of GO lens.

According to the optical profiler measurement (Fig. 2(c)) and AFM image (Fig. 2(d)), the thickness fluctuation is approximately 10%. Using the same method to calculate the amplitude and phase modulations, we can get the corresponding maximum and minimum amplitude and phase modulations.

Appendix Table S1 | The influence of GO film thickness on optical modulation

GO thickness	GO Amplitude	RGO Amplitude	Phase modulation
200 nm	0.8567	0.5949	0.1700π
220 nm	0.8436	0.5648	0.1870π
180 nm	0.8701	0.6266	0.1530π

Because of the fluctuation of GO film thickness, the phase and amplitude modulations are not as accurate as the designs, which will break the interference condition of both GO metalenses. In this way, the optical characterization in Fig. 3 and Fig. 4 do not exactly match the designs. However, for real application, the quality of the generated optical needle and multifocal array is reasonably good.

On the other hand, defects and particles on GO film will also compromise the interference condition, especially in the case of the multifocal metalens, and thus contribute to the discrepancy between the design and the experimental result of the far field intensity patterns in Fig. 3 and Fig. 4.

S 2.1 Geometric tables of axial multifocal GO metalens

Appendix Table S2 | Geometry of the 350μm axial multifocal GO metalens

n	R_n(μm)	n	R_n(μm)	n	R_n(μm)	n	R_n(μm)
1	16.48	26	83.25	51	120.40	76	150.28
2	22.87	27	84.89	52	121.65	77	151.37
3	27.84	28	86.51	53	122.90	78	152.45
4	32.06	29	88.10	54	124.14	79	153.53
5	35.80	30	89.67	55	125.37	80	154.60
6	39.20	31	91.55	56	126.60	81	156.01
7	42.33	32	93.08	57	127.81	82	157.07
8	45.25	33	94.59	58	129.01	83	158.13
9	48.01	34	96.08	59	130.21	84	159.18
10	50.62	35	97.55	60	131.40	85	160.24
11	53.44	36	99.00	61	132.58	86	161.28
12	55.85	37	100.44	62	133.75	87	162.32
13	58.16	38	101.86	63	134.92	88	163.36
14	60.38	39	103.27	64	136.08	89	164.39
15	62.54	40	104.65	65	137.23	90	165.42
16	64.63	41	106.59	66	138.38	91	167.32
17	66.66	42	107.96	67	139.52	92	168.35
18	68.64	43	109.31	68	140.65	93	169.37
19	70.56	44	110.65	69	141.78	94	170.39
20	72.44	45	111.98	70	142.90	95	171.40
21	74.56	46	113.30	71	144.77	96	172.41
22	76.37	47	114.60	72	145.88	97	173.42
23	78.14	48	115.90	73	146.99	98	174.42
24	79.87	49	117.18	74	148.09	99	175.42
25	81.57	50	118.45	75	149.19	100	176.42

S 2.2 Geometric tables of optical needle GO metalens

Appendix Table S3 | Geometry of the 350μm optical needle GO metalens

n	R_n(μm)	n	R_n(μm)	n	R_n(μm)	n	R_n(μm)
1	16.48	26	83.44	51	119.59	76	148.99
2	22.87	27	85.09	52	120.84	77	150.07
3	27.84	28	86.71	53	122.08	78	151.14
4	32.06	29	88.30	54	123.31	79	152.21
5	35.80	30	89.88	55	124.54	80	153.27
6	39.20	31	91.77	56	125.75	81	154.58
7	42.33	32	93.31	57	126.96	82	155.64
8	45.25	33	94.82	58	128.15	83	156.69
9	48.01	34	96.31	59	129.34	84	157.74
10	50.62	35	97.79	60	130.53	85	158.78
11	53.44	36	99.24	61	131.96	86	159.82
12	55.85	37	100.68	62	133.13	87	160.85
13	58.16	38	102.11	63	134.29	88	161.88
14	60.38	39	103.51	64	135.45	89	162.91
15	62.54	40	104.91	65	136.60	90	163.93
16	64.63	41	106.28	66	137.74	91	165.24
17	66.66	42	107.65	67	138.87	92	166.25
18	68.64	43	109.00	68	140.00	93	167.26
19	70.56	44	110.34	69	141.12	94	168.27
20	72.44	45	111.66	70	142.24	95	169.28
21	74.73	46	112.97	71	143.52	96	170.28
22	76.54	47	114.28	72	144.62	97	171.27
23	78.32	48	115.57	73	145.72	98	172.27
24	80.06	49	116.85	74	146.82	99	173.26
25	81.76	50	118.12	75	147.91	100	174.25

S 3 Femtosecond Laser fabrication setup

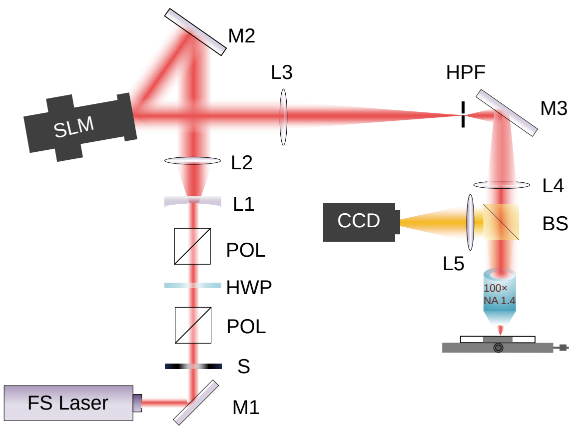

Appendix Fig. S4 | Schematic of experimental setup of the femtosecond laser nanofabrication system. The femtosecond laser is Libra from Coherent®. Its pulse width, repetition rate and wavelength are 100 fs, 100 kHz and 800 nm respectively. M, mirror; S, shutter; POL, polarizer; HWP, half wave plate; HPF, high pass filter; BS, beam splitter.

S 4 Focusing characterization setup

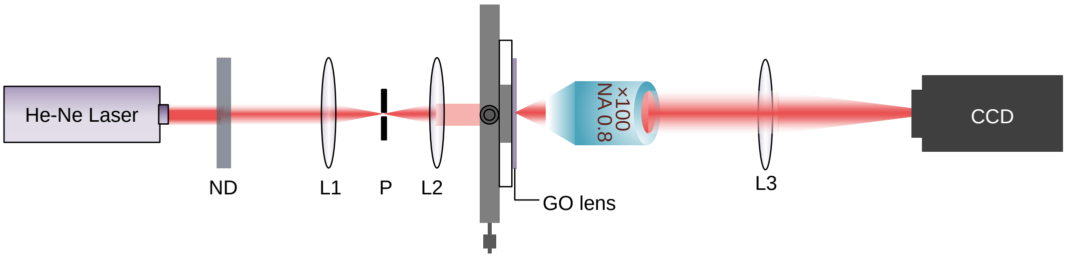

Appendix Fig. S5 | Schematic of experimental setup for focusing characterization setup. ND, Neutral density filter; P, pinhole. L1, P and L2 achieve the function of spatial filtering. The objective and L3 consist a 4*f* system.

References

1. Zheng X, Jia B, Chen X, Gu M. *Adv Mater* **26**, 2699–703 (2014).
2. Bass M, Stryland EWV, Williams DR, Wolfe WL. 1995